Research Article | Vol. 14, No. 4 / 1 Apr 2023 / Biomedical Optics Express 1472
Biomedical Optics EXPRESS

Temperature dependence of the dielectric function of dehydrated biological samples in the THz band

JAN HELMINIAK,[1] MARIANA ALFARO-GOMEZ,[2] GORETTI G. HERNANDEZ-CARDOSO,[1] MARTIN KOCH,[1] AND ENRIQUE CASTRO-CAMUS[1,*]

[1]Department of Physics and Material Sciences Center, Philipps-Universität Marburg, Renthof 5, 35032 Marburg, Germany
[2]Universidad Autonoma de Aguascalientes, Av. Universidad 940, Cd. Universitaria, 20100, Aguascalientes, Mexico
[*]enrique.castrocamus@physik.uni-marburg.de

Abstract: Terahertz technology has demonstrated enormous potential for the analysis of biological systems and the diagnosis of some medical conditions, given its high sensitivity to detect water content. In previously published papers, effective medium theories are used to extract the water content from the terahertz measurements. When the dielectric functions of water and dehydrated bio-material are well known, the volumetric fraction of water can be left as the only free parameter in those effective medium theory models. While water complex permittivity is very well known, the dielectric functions of dehydrated tissues are normally measured for each individual application. In previous studies, it has been traditionally assumed that, unlike water, the dielectric function of the dehydrated tissues is temperature independent, measuring it only at room temperature. Yet, this is an aspect that has not been discussed and that is relevant in order to get THz technology closer to clinical and in-the-field applications. In this work, we present the characterization of the complex permittivity of dehydrated tissues; each studied at temperatures ranging from 20°C to 36.5°C. We studied samples of different organism classifications to have a wider confirmation of the results. We find that, in each case, the dielectric function changes of dehydrated tissues caused by temperature are smaller than for water across the same temperature interval. Yet, the changes in the dielectric function of the dehydrated tissue are not negligible and should, in many cases, be taken into account for the processing of terahertz signals that interact with biological tissues. While this study gives a first introduction into the probable relevancy of temperature-dependent optical behavior of biological samples, this work only focuses on the experimental proof for this relationship and will, therefore, not give a deeper analysis of how the underlying models have to be modified.

1. Introduction

In the last three decades, terahertz radiation has met a wide set of applications. The field is growing rapidly thanks to a very active scientific community [1–4]. In particular, many review articles have remarked the importance and impact of terahertz technology for biological and medical applications [5–14]. Most of these research aims to determine the water content of a sample, using the results to draw further conclusions regarding its biological state. The water content is measured by calculating the dielectric function of the sample and using effective medium theory to quantify the volume of water within a sample. For instance, excised cancerous tissue exhibits clear contrast to healthy one because of its higher water content and higher values of the dielectric function [15,16]. *In-vivo* applications of skin measurements have also shown how changes on the dielectric function can be used to study different conditions, such as diabetic

#478787 https://doi.org/10.1364/BOE.478787
Journal © 2023 Received 19 Oct 2022; revised 25 Jan 2023; accepted 25 Jan 2023; published 8 Mar 2023

Biomedical Optics EXPRESS

foot [17], burn severity [18,19] or scar treatment [20]. In the biological field, measuring the state of hydration of plant leaves through the dielectric function has also led to understanding important biological behaviour such as responses to light or drought stress [21–25].

Biological systems are in general heterogeneous in nature. In the THz band, they can be studied as a mixture of different materials modeled with effective medium theory. In these models, the dielectric function is calculated using the volumetric fractions and the individual dielectric properties of the sample components [26,27]. For example, the Landau-Lifschitz-Looyenga model, which is commonly used for THz analysis, assumes a non-linear superposition of the dielectric functions of the components that gives the dielectric function of the mixed hydrated tissue. With this model, a biological sample is most commonly assumed as a composition of water, dehydrated material and air. In materials such as skin, which have higher density in the dehydrated part, the air contribution can be sometimes neglected. In most of such studies, the temperature dependent dielectric function of water is obtained from a well established Double-Debye model [28], while the dielectric function of dried tissue is experimentally characterized, usually at room temperature, neglecting any influences of the temperature. As THz technology targets and gets closer to clinical applications, it is important to analyze all the variables that may give possible measurement deviations, temperature being one of them. As mentioned earlier, dehydrated samples are usually characterized at room temperature, however, many living organisms, including humans, regulate their own temperature. This means that individuals may present different body temperatures and even change their own temperature during a diagnostic test procedure. Therefore, it is important to know how the non-water component of a tissue may change its dielectric function for different temperatures. Here, we investigate the possible temperature dependence of the dielectric function for various dehydrated biological samples of different nature and discuss the implication of the results for the biological applications of THz technology. Our main objective is to provide evidence that there is a non-negligible dependence of the dielectric function of the non-water part of the tissue, but by no means to provide quantitative rule that is generally applicable to tissues, since each particular dehydrated tissue will have to be characterized in future studies accordingly.

2. Materials and methods

2.1. Biological samples

We considered the analysis of three biological samples from different organism classifications in our study as shown in Fig. 1(a). The first sample was porcine skin tissue, which is an accepted model of human skin [29,30]. The second sample was an oak leaf (*Quercus robur)* and the last one was a mushroom sample (*Agaricus bisporus*). Tissue samples were put first into a Formaldehyde-solution for 24 hours to avoid cellular decomposition and retain their original structure [31,32]. After this, the samples were dehydrated using ethanol baths ranging from 20 to 60 min, depending on their thickness. The main dehydration process included successively increasing ethanol concentrations in the order: 70%, 80%, 90%, 95%, and 100%. After the 100% concentration bath, we dried the samples in the oven at 40°C for at least 24 h to ensure no ethanol is left for THz measurements and to reassure the dehydration status.

2.2. Temperature controlled chamber

During the spectroscopic measurements, the samples were placed in a self-designed and constructed temperature-controlled chamber to study the possible temperature dependence of their dielectric properties as shown in Fig. 1(b). The chamber was designed to regulate temperatures between room temperature (~20°C) and 40°C. For this purpose, two resistors (R) were attached to the aluminum housing forming the main heating system. The resistors temperatures were regulated proportionally to an applied electrical voltage (V_0). An Arduino

Biomedical Optics EXPRESS

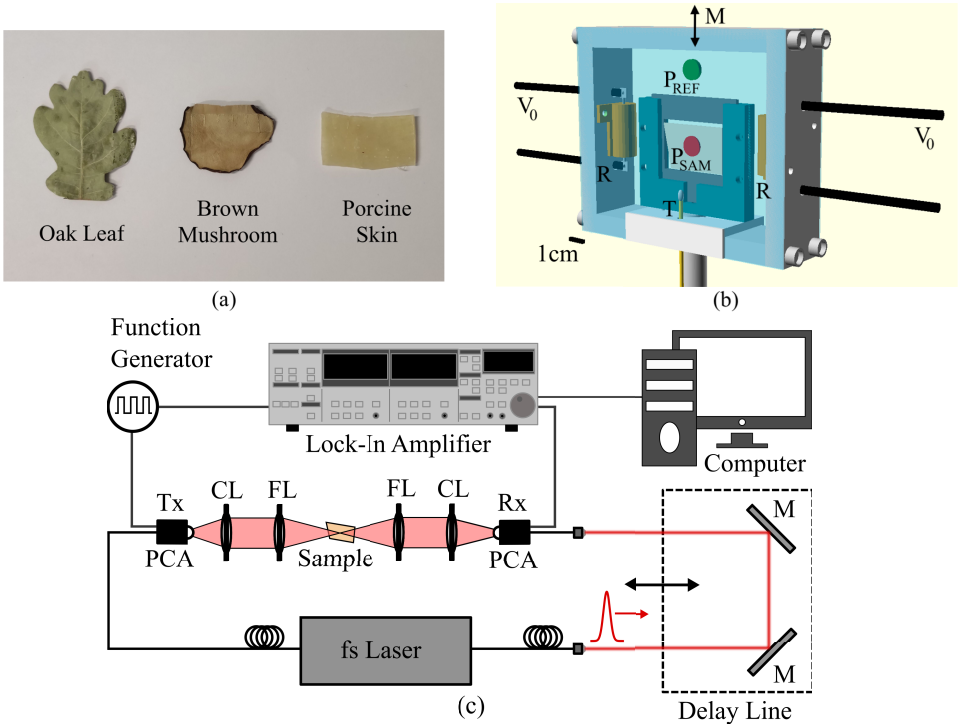

Fig. 1. (a) Biological samples from different organism classifications after dehydration process. The samples are (from left to right) oak leaf (*Quercus robur)*, brown mushroom (*Agaricus bisporus*) and porcine skin tissue. (b) Design of the heat chamber (height × width × depth = 10.5 × 12.5 × 3.0 cm with 1.0 cm wall thickness). V_0 indicates the voltage supply, R are the resistors, H is the sample holder, M indicates linear movement for sample (red) and reference (green) focus P of the THz beam. (c) Schematically representation of the terahertz time-domain transmission set-up used for the measurement series.

ONE micro-controller monitored the temperature in the chamber and controlled the current flowing through the resistors. The temperature data was continuously acquired with a thermistor (T) placed near the sample. The resistors were turned on or off by switching a relay after comparing the measured to the target temperature. To ensure that the sample itself holds the target temperature, the target temperature was kept constant for a few minutes to guarantee thermal equilibrium of the chamber and the sample. To keep the heat inside the chamber and to allow the penetration of both THz radiation and nitrogen into the cavity, each side was covered by a window made of thin plastic foil.

2.3. THz time-domain measurements

We used the previously described cavity in combination with a standard transmission terahertz time-domain spectrometer as shown in Fig. 1(c). Terahertz radiation was created and detected by overlapping femtosecond laser pulses together with an external electrical DC signal on two photoconductive antennae with 2 THz bandwidth. The heat chamber was mounted on a translation stage allowing us to acquire sample and reference signals by linearly moving the unit (M) to reference (P_{Ref}) and sample (P_{Sam}) positions as shown in Fig. 1(b). By choosing to place the reference measurement (P_{Ref}) inside the cavity, the influences from the plastic foil and the current environmental conditions could be compensated for. The measurements were made under

Biomedical Optics EXPRESS

nitrogen atmosphere to improve the signal-to-noise ratio (SNR) and avoid the spectral features of water vapour.

The complex refractive index $\tilde{n}(\omega)$ and the dielectric function $\epsilon(\omega)$ were related through $\epsilon(\omega) = \tilde{n}^2$, where $\tilde{n}(\omega) = n(\omega) + i\kappa(\omega)$, with $n(\omega)$ the refractive index and $\kappa(\omega)$ the extinction coefficient. These were calculated using the Fourier transforms of the measured electric field waveforms for reference and sample ($\tilde{T}(\omega) = \tilde{E}_{\text{sam}}(\omega)/\tilde{E}_{\text{ref}}(\omega)$) and the theoretical Fresnel transmission ($\tilde{T} = t_{12}(\omega)t_{21}(\omega)e^{i\frac{d\omega}{c}(\tilde{n}(\omega)-1)}$). From this,

$$n(\omega) = 1 + \frac{c}{\omega d}\left(\phi_{\text{sam}}(\omega) - \phi_{\text{ref}}(\omega)\right), \tag{1}$$

$$\kappa(\omega) = -\frac{c}{2d\omega}\ln\left(\frac{1}{t_{12}t_{21}}\frac{\varepsilon_{\text{sam}}(\omega)}{\varepsilon_{\text{ref}}(\omega)}\right), \tag{2}$$

where $\phi(\omega)$ and $\varepsilon(\omega)$ are the phase and amplitude of $\tilde{E}_{sam}(\omega)$ and $\tilde{E}_{ref}(\omega)$. Then, the real and imaginary parts of the dielectric function were calculated as $\epsilon'(\omega) = n(\omega)^2 - \left(\frac{c\alpha(\omega)}{2\omega}\right)^2$ and $\epsilon''(\omega) = 2n(\omega)\kappa(\omega)$, respectively.

For each biological specimen type, the dielectric function was analyzed under temperature conditions of 20°C, 22.5°C, 27.5°C, 32.5°C, and 36.5°C. Five samples for each kind of tissue where used and measured independently, the error bars shown in the plots represent the standard deviation of the five measurements. We limited our analysis to the frequency interval of 0.2 THz to 1 THz, where the signal-to-noise ratio of our set-up is highest.

3. Results and discussion

The real and imaginary parts of the dielectric functions of dehydrated samples of porcine skin, oak leaf and mushroom are shown in Fig. 2.(a)-(c), respectively, for a temperature interval from 20°C to 36.5°C as we show, together with additional parameters, in Dataset 1, (Ref. [33]) Dataset 2, (Ref. [34]) and Dataset 3, (Ref. [35]). Notice that all spectra show a soft and continuous shape, without prominent features. When we compare the actual values for porcine skin, oak leaf and mushroom samples, we see large differences among them, which we believe, may be mostly attributed to their different densities with values of 998±20 kg/m^3, 544±70 kg/m^3, and 359±60 kg/m^3, respectively. These density values were measured directly from our samples. As a point of comparison, the dielectric function of water from the Double-Debye model is shown in Fig. 2(d), depicting a much more pronounced dependence with temperature. The dielectric function at 500 GHz for the temperature intervals, as well as a linear fit are shown in Fig. 3. The slope of the linear fit gives the rate of change of the dielectric function with respect to temperature. The slope values for each fit are shown in Table 1.

Table 1. Change of real and imaginary parts of the dielectric function with respect to temperature for the bio-samples and water. The values are the slopes of the linear fits presented in Fig. 3. The last column shows the densities of the biological tissues calculated for each tissue type, determined by measuring the volume and mass for each sample.

Bio-sample	$d\epsilon'/dT$ [ϵ_0/°C]	$d\epsilon''/dT$ [ϵ_0/°C]	Densities [kg/m^3]
Porcine skin	-6.79×10^{-3}	3.2×10^{-3}	998 (± 20)
Oak Leaf	-1.72×10^{-3}	-8.602×10^{-4}	544 (± 70)
Brown Mushroom	-1.709×10^{-3}	1.86×10^{-4}	359 (± 60)
Water	1.09×10^{-2}	2.8×10^{-2}	997

Biomedical Optics EXPRESS

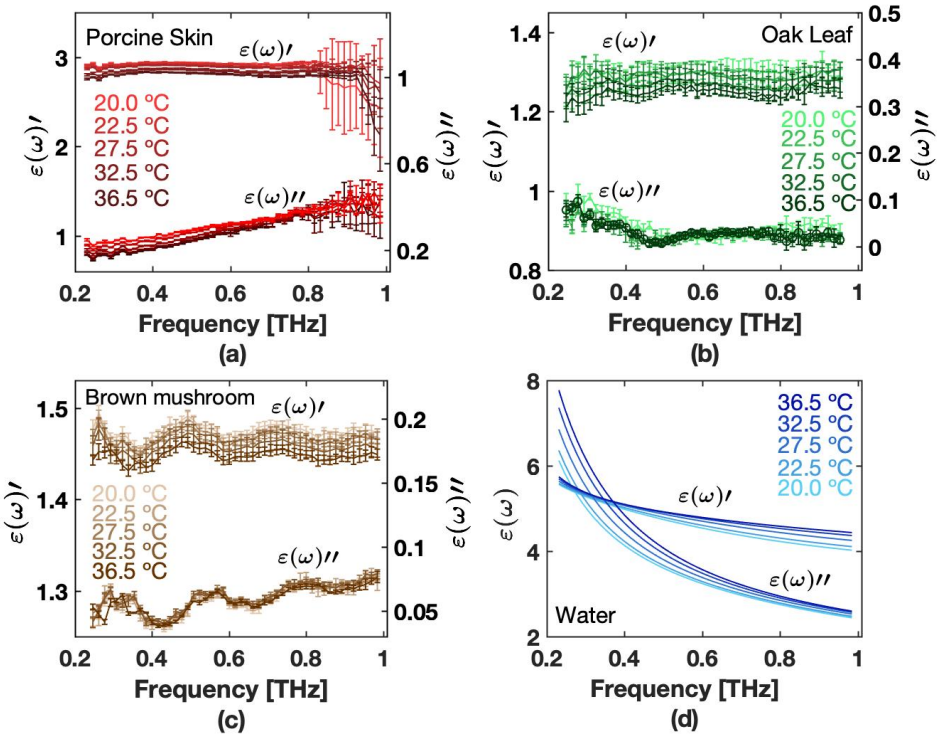

Fig. 2. Real and imaginary parts of the dielectric function of dehydrated (a) porcine skin, (b) oak leaf, (c) brown mushroom and (d) water for different temperatures in a frequency range of 0.2 THz to 1 THz.

Until now, most THz analyses of biological samples had assumed that the dielectric function of dry tissue would have little or no temperature dependence. This assumption implies that any temperature dependence would be attributed only to the dielectric function of water. From the results shown in Fig. 3(a)-(d), it can be seen that the change in dielectric function for the dehydrated tissues is less than that of water at 500 GHz, yet not entirely negligible. Furthermore, while changes of the imaginary part of the dielectric function of water are higher at lower frequencies, the changes in the tissue samples appear to be less frequency-dependent.

The results confirm that temperature changes on the dielectric function of dehydrated samples should be taken into account in order to improve the accuracy of the results. While we do not think that qualitative behaviour inferred from previous studies or their general conclusions would be significantly different, the accuracy of the quantitative part of some of them might need to be re-discussed. The experiment was performed with animal, vegetative and fungal tissues, covering a variety of tissue types of potential interest for future THz biological and biomedical applications.

Biomedical Optics EXPRESS

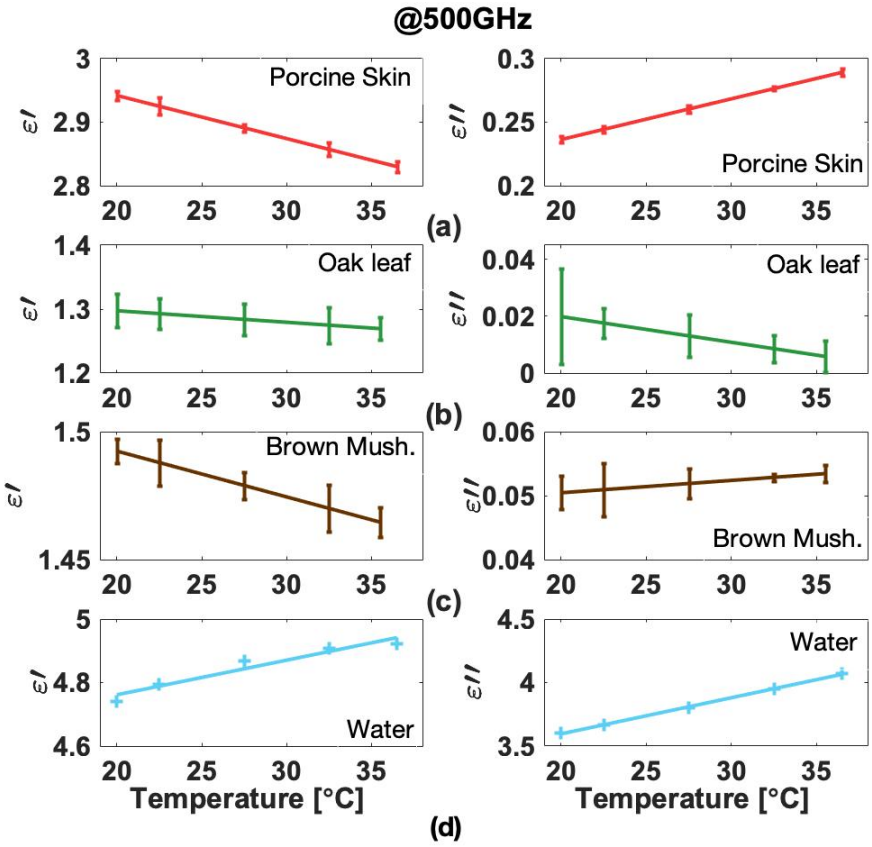

Fig. 3. Changes of the real part (left column) and the imaginary part (right column) of the dielectric function at 500 GHz for dehydrated (a) porcine skin, (b) oak leaf, (c) brown mushroom and (d) water.

4. Conclusions

We characterized the dielectric function of dehydrated samples of pig skin, plant leaves and mushroom under different temperatures. Our results confirm that changes on the dielectric function of dehydrated biological samples are smaller than that of water but not always negligible, an example is porcine skin, which shows a significant effect. This implies that biological and biomedical samples might need to take this into account in order to be trustfully modeled through effective medium theory.

Funding. Philipps-Universität Marburg; Universidad Autónoma de Aguascalientes (PIM19-6N); Consejo Nacional de Ciencia y Tecnología (A1-S-37249); Alexander von Humboldt-Stiftung.

Disclosures. The authors declare no conflicts of interest.

Data availability. Data underlying the results presented in this paper are not publicly available at this time but may be obtained from the authors upon reasonable request.

The calculated dielectric functions shown in this study and additional obtained parameters as the real and imaginary part of the refractive index, the absorption coefficient, the real and imaginary part of the dielectric function plus their statistical errors for each temperature and specimen type are available in the Dataset 1, (Ref. [33]) Dataset 2, (Ref. [34]) and Dataset 3, (Ref. [35]).

Biomedical Optics EXPRESS

References

1. S. S. Dhillon, M. S. Vitiello, and E. H. Linfield, "The 2017 terahertz science and technology roadmap," Journal of Physics D: Applied Physics **50**, 043001 (2017).
2. S. Das, N. Anveshkumar, J. Dutta, and A. Biswas, *Advances in Terahertz Technology and Its Applications* (Springer, 2021).
3. J. Hesler, R. Prasankumar, and J. Tignon, "Advances in terahertz solid-state physics and devices," Journal of Applied Physics **126**, 110401 (2019).
4. K. Sengupta, T. Nagatsuma, and D. M. Mittleman, "Terahertz integrated electronic and hybrid electronic–photonic systems," Nature Electronics **1**, 622–635 (2018).
5. X. Chen, H. Lindley-Hatcher, R. I. Stantchev, J. Wang, K. Li, A. Hernandez Serrano, Z. D. Taylor, E. Castro-Camus, and E. Pickwell-MacPherson, "Terahertz (thz) biophotonics technology: Instrumentation, techniques, and biomedical applications," Chem. Phys. Rev. **3**, 011311 (2022).
6. S. Khushbu, M. Yashini, R. Ashish, and C. K. Sunil, "Recent advances in terahertz time-domain spectroscopy and imaging techniques for automation in agriculture and food sector," Food Analytical Methods **15**, 498–526 (2022).
7. A. I. Nikitkina, P. Bikmulina, E. R. Gafarova, N. V. Kosheleva, Y. M. Efremov, E. A. Bezrukov, D. V. Butnaru, I. N. Dolganova, N. V. Chernomyrdin, O. P. Cherkasova, A. A. Gavdush, and P. S. Timashev, "Terahertz radiation and the skin: a review," Journal of Biomedical Optics **26**, 1–26 (2021).
8. Q. Sun, Y. He, K. Liu, S. Fan, E. P. J. Parrott, and E. Pickwell-MacPherson, "Recent advances in terahertz technology for biomedical applications," Quantitative Imaging in Medicine and Surgery **7**(3), 345–355 (2017).
9. C.-H. Feng and C. Otani, "Terahertz spectroscopy technology as an innovative technique for food: current state-of-the-art research advances," Critical Reviews in Food Science and Nutrition **61**, 2523–2543 (2021). PMID: 32584169.
10. L. Yu, L. Hao, T. Meiqiong, H. Jiaoqi, L. Wei, D. Jinying, C. Xueping, F. Weiling, and Z. Yang, "The medical application of terahertz technology in non-invasive detection of cells and tissues: opportunities and challenges," RSC Adv. **9**, 9354–9363 (2019).
11. K. Ahi, N. Jessurun, M.-P. Hosseini, and N. Asadizanjani, "Survey of terahertz photonics and biophotonics," Optical Engineering **59**, 1–31 (2020).
12. L. Wei, L. Yu, H. Jiaoqi, H. Guorong, Z. Yang, and F. Weiling, "Application of terahertz spectroscopy in biomolecule detection," Frontiers in Laboratory Medicine **2**, 127–133 (2018).
13. A. Gong, Y. Qiu, X. Chen, Z. Zhao, L. Xia, and Y. Shao, "Biomedical applications of terahertz technology," Applied Spectroscopy Reviews **55**, 418–438 (2020).
14. A. Ren, A. Zahid, D. Fan, X. Yang, M. A. Imran, A. Alomainy, and Q. H. Abbasi, "State-of-the-art in terahertz sensing for food and water security –a comprehensive review," Trends in Food Science & Technology **85**, 241–251 (2019).
15. K. I. Zaytsev, I. N. Dolganova, N. V. Chernomyrdin, G. M. Katyba, A. A. Gavdush, O. P. Cherkasova, G. A. Komandin, M. A. Shchedrina, A. N. Khodan, D. S. Ponomarev, I. V. Reshetov, V. E. Karasik, M. Skorobogatiy, V. N. Kurlov, and V. V. Tuchin, "The progress and perspectives of terahertz technology for diagnosis of neoplasms: a review," Journal of Optics **22**, 013001 (2019).
16. Y. Peng, C. Shi, X. Wu, Y. Zhu, and S. Zhuang, "Terahertz imaging and spectroscopy in cancer diagnostics: a technical review," BME Frontiers **2020**, 2547609 (2020).
17. G. G. Hernandez-Cardoso, L. F. Amador-Medina, G. Gutierrez-Torres, E. S. Reyes-Reyes, C. A. Benavides Martínez, C. Cardona Espinoza, J. Arce Cruz, I. Salas-Gutierrez, B. O. Murillo-Ortíz, and E. Castro-Camus, "Terahertz imaging demonstrates its diagnostic potential and reveals a relationship between cutaneous dehydration and neuropathy for diabetic foot syndrome patients," Scientific Reports **12**, 3110 (2022).
18. Z. D. Taylor, R. S. Singh, M. O. Culjat, J. Y. Suen, W. S. Grundfest, H. Lee, and E. R. Brown, "Reflective terahertz imaging of porcine skin burns," Optics Letters **33**, 1258–1260 (2008).
19. M. H. Arbab, D. P. Winebrenner, T. C. Dickey, A. Chen, M. B. Klein, and P. D. Mourad, "Terahertz spectroscopy for the assessment of burn injuries *in vivo*," Journal of Biomedical Optics **18**, 077004 (2013).
20. J. Wang, Q. Sun, R. I. Stantchev, T.-W. Chiu, A. T. Ahuja, and E. Pickwell-MacPherson, "In vivo terahertz imaging to evaluate scar treatment strategies: silicone gel sheeting," Biomedical Optics Express **10**, 3584–3590 (2019).
21. A. K. Singh, A. V. Pérez-López, J. Simpson, and E. Castro-Camus, "Three-dimensional water mapping of succulent agave Victoriae-Reginae leaves by terahertz imaging," Scientific Reports **10**, 1404 (2020).
22. N. Born, D. Behringer, S. Liepelt, S. Beyer, M. Schwerdtfeger, B. Ziegenhagen, and M. Koch, "Monitoring plant drought stress response using terahertz time-domain spectroscopy," Plant physiology **164**, 1571–1577 (2014).
23. M. Browne, N. T. Yardimci, C. Scoffoni, M. Jarrahi, and L. Sack, "Prediction of leaf water potential and relative water content using terahertz radiation spectroscopy," Plant Direct **4**, e00197 (2020).
24. F. V. Di Girolamo, M. Pagano, A. Tredicucci, M. Bitossi, R. Paoletti, G. P. Barzanti, C. Benvenuti, P. F. Roversi, and A. Toncelli, "Detection of fungal infections in chestnuts: a terahertz imaging-based approach," Food Control **123**, 107700 (2021).
25. E. Castro-Camus, M. Palomar, and A. A. Covarrubias, "Leaf water dynamics of arabidopsis thaliana monitored in-vivo using terahertz time-domain spectroscopy," Scientific Reports **3**, 2910 (2013).

Biomedical Optics EXPRESS

26. G. G. Hernandez-Cardoso, A. K. Singh, and E. Castro-Camus, "Empirical comparison between effective medium theory models for the dielectric response of biological tissue at terahertz frequencies," Applied Optics **59**, D6–D11 (2020).
27. M. Borovkova, M. Khodzitsky, P. Demchenko, O. Cherkasova, A. Popov, and I. Meglinski, "Terahertz time-domain spectroscopy for non-invasive assessment of water content in biological samples," Biomed Opt Express **9**, 2266–2276 (2018).
28. H. J. Liebe, G. A. Hufford, and T. Manabe, "A model for the complex permittivity of water at frequencies below 1 thz," International Journal of Infrared and Millimeter Waves **12**, 659–675 (1991).
29. N. Sekkat, Y. N. Kalia, and R. H. Guy, "Biophysical study of porcine ear skin in vitro and its comparison to human skin in vivo," Journal of Pharmaceutical Sciences **91**, 2376–2381 (2002).
30. C. Herkenne, A. Naik, Y. N. Kalia, J. Hadgraft, and R. H. Guy, "Pig ear skin ex vivo as a model for in vivo dermatopharmacokinetic studies in man," Pharmaceutical Research **23**, 1850–1856 (2006).
31. A. Mehdizadeh Kashi, K. Tahemanesh, S. Chaichian, M. T. Joghataei, F. Moradi, S. M. Tavangar, A. S. Mousavi Najafabadi, N. Lotfibakhshaiesh, S. Pour Beyranvand, A. Fazel Anvari-Yazdi, and S. M. Abed, "How to prepare biological samples and live tissues for scanning electron microscopy (sem)," Galen Medical Journal **3**, 63–80 (2014).
32. Yiwen Sun, Bernd M Fischer, and Emma Pickwell-MacPherson, "Effects of formalin fixing on the terahertz properties of biological tissues," J. Biomed. Opt. **14**, 064017 (2009).
33. J. Helminiak, "Brown mushroom data," figshare, (2022), https://doi.org/10.6084/m9.figshare.21647756.v1.
34. J. Helminiak, "Oak leaf data," figshare, (2022), https://doi.org/10.6084/m9.figshare.21647759.v1.
35. J. Helminiak, "Porcine skin data," figshare, (2022), https://doi.org/10.6084/m9.figshare.21647762.v1.